Analytical and Bioanalytical Chemistry
https://doi.org/10.1007/s00216-020-02928-7

RESEARCH PAPER

A sensitive biosensor for determination of pathogenic bacteria using aldehyde dehydrogenase signaling system

Wenguang Zhang[1,2] · Shengjun Bu[2] · Huasong Bai[2] · Chengyou Ma[3] · Li Ma[2] · Hongguo Wei[2] · Xiu Liu[2] · Zehong Li[1] · Jiayu Wan[2]

Received: 30 June 2020 / Revised: 4 August 2020 / Accepted: 28 August 2020

Abstract

Aldehyde dehydrogenase (ALDH) was first developed as an enzymatic signaling system of a biosensor for sensitive point-of-care detection of pathogenic bacteria. ALDH and specific aptamers to *Salmonella typhimurium* (*S. typhimurium*), as organic components, were embedded in organic-inorganic nanocomposites as a biosensor signal label, integrating the functions of signal amplification and target recognition. The biosensing mechanism is based on the fact that ALDH can catalyze rapid oxidation of acetaldehyde into acetic acid, resulting in pH change with portable pH meter readout. The altered pH exhibited a linear relationship with the logarithm of *S. typhimurium* from 10^2 to 10^8 CFU/mL and detection limit of 46 CFU/mL. Thus, the proposed biosensor has potential application in the diagnosis of pathogenic bacteria.

Keywords *Salmonella typhimurium* · Aldehyde dehydrogenase · Nanocomposite · pH meter

Introduction

Point-of-care (POC) diagnostic technology with high performance is becoming increasingly popular, playing a vital role in maintaining a healthy society and food safety [1, 2]. Qualitative or quantitative detection of clinically relevant biological targets, such as small molecules, proteins, nucleic acids, and pathogens, is of crucial significance for improving the level of diagnosis, timely and effective treatment of diseases, and prevention of pathogen infection [3]. Among these approaches, biosensors with the functions of target-specific recognition and signal transduction play an important prominent role [4]. Biosensors convert biorecognition element of binding to its target into physicochemical detection signals [5]. To facilitate the use of biosensors at POC locations, several physiochemical detectable signals, including glucose [6], pressure [7], temperature [8], hydrogen [9], and electrochemical signal [10], are used as readouts. These signal transduction strategies revamp the commercially available hand-held meters, such as personal glucose meter (PGM), pressure meter, thermometer, hydrogen detector, and screen-printed carbon electrodes [11]. Smartphone has also been used as a low-cost hand-held reader for POCT [12, 13]. When combined with biochemical analysis, these commercial hand-held devices can be employed for POC testing of a wide variety of targets. It must be noted that these biosensors require a signaling system to generate signals for hand-held meters used in POC testing. For instance, the PGM converts a substrate to glucose mainly based on enzymatic signaling system. There are several classes of enzymes, such as invertase [14], glucoamylase [15], hexokinase [16], galactosidase [17], and alkaline phosphatase [18], which have been shown to produce glucose from a variety of substrates. Numerous catalysts, such as catalase [19], platinum nanoparticles [20], and CuO/Co_3O_4 heterojunction nanofibers [21, 22], have been explored as enzymatic signaling system to catalytically decompose substrate for the generation of gas in closed system by using a cheap and

Electronic supplementary material The online version of this article (https://doi.org/10.1007/s00216-020-02928-7) contains supplementary material, which is available to authorized users.

✉ Zehong Li
554233128@qq.com

✉ Jiayu Wan
wanjiayu@hotmail.com

[1] College of Life Science, Jilin Agricultural University, Changchun 130118, Jilin, China

[2] Institute of Military Veterinary, Academy of Military Medical Sciences, Changchun 130122, Jilin, China

[3] College of Geo-Exploration Science and Technology, Jilin University, Changchun 130026, Jilin, China

Published online: 02 September 2020

portable gas pressure meter as readout. Based on portable thermometer to read signal, the photo-heat conversion materials, such as graphene oxides [23], are usually used as the signal amplification platform [24, 25]. Platinum nanoparticles can efficiently catalyze the dissolution of ammonia borane complex to generate hydrogen gas with hand-held hydrogen detector meter readout [9].

In recent years, hand-held pH meters, with the advantages of low cost and simple operation, have been developed for measuring the pH of solutions [26]. Based on the pH meter as a signal reading tool, fabricated biosensors had been applied to a variety of targets, such as mycotoxin [27], proteins [28, 29], DNA sequences [30], and bacterial pathogens [31]. Enzymes, such as acetylcholine esterase [26], glucose oxidase [31], alkaline phosphatase [18], and urease [32], which could effectively catalyze their corresponding substrates to cause changes in the solution pH, have been developed as powerful tags of these fabricated biosensors. Therefore, the enzyme activity as the signal label and sensitivity of the pH meter determine the analytical performance of a biosensor.

Acetaldehyde dehydrogenase (ALDH) is an important class of enzyme which oxidizes aldehydes to their corresponding carboxylic acids [33]. As a crucial regulator of aldehyde metabolism in the human body, ALDH can effectively protect the body from active aldehydes [34]. Several acetaldehyde biosensors have been constructed for the detection of acetaldehyde in mixture solution or gas using ALDH. For instance, Avramescu et al. developed amperometric biosensor using ALDH for the determination of acetaldehyde to control wine quality [35], while Iitani et al. constructed fiber optic biosensors for the measurement of acetaldehyde in liquid phase using ALDH [36]. Furthermore, bioelectronic gas sensors incorporating ALDH have been developed for convenient analysis of acetaldehyde in expired gas [37], and a stick-type biochemical gas sensor with ALDH has been developed for convenient analysis of breath acetaldehyde [38]. However, to the best of our knowledge, ALDH-catalyzed rapid oxidation of acetaldehyde to form acetic acid has not yet been applied as a signal output in immunosensors.

A novel nanocomposite with phosphate as inorganic component and protein as organic component has attracted widespread attention in the field of biosensors owing to its large surface area, good stability, and simple preparation [39]. The nanocomposite can improve the catalytic activity and durability of the organic component (protein). Multiple proteins are embedded in nanocomposites with several integrated functions [40]. Ye et al. developed a POC biosensor based on concanavalin A-glucose oxidase-$CaHPO_4$ organic-inorganic nanocomposites as signal tags and a hand-held pH meter signal readout. Glucose oxidase–embedded nanocomposites can efficiently convert glucose to gluconic acid, which causes a decrease in the pH [31]. Ye et al. prepared concanavalin A-invertase-$CaHPO_4$ integrating both essential functions of biological recognition and signal amplification for POC testing of *Escherichia coli* O157:H7 [41]. Bai et al. synthesized antimicrobial peptides-invertase-$Ca_3(PO_4)_2$ organic-inorganic nanocomposites with multifunctional target recognition and signal transduction for POC determination of pathogenic bacteria [42]. As a signal output, the invertase in the nanocomposites hydrolyzes sucrose to glucose, which can be reliably quantified on a PGM.

We first established a portable biosensor based on ALDH-aptamer-$Ca_3(PO_4)_2$ organic-inorganic hybrid nanocomposite (AAC), as a signal probe and pH meter as a readout (Scheme 1). The pathogenic bacterium, *S. typhimurium*, was used as the detection model. AAC was synthesized by a simple one-step process using ALDH and Salmonella-specific aptamer as organic materials and calcium phosphate as inorganic material. Ferroferric oxide (Fe_3O_4)-embedded aptamer-$Ca_3(PO_4)_2$ hybrid nanocomposite (FAC) was exploited as the magnetic capture probe for the isolation of *S. typhimurium*. In the presence of *S. typhimurium*, a sandwich complex was formed between capture probe AAC and signal probe FAC. The ALDH in the sandwich immunocomplex catalyzed conversion of acetaldehyde into acetic acid. The generated acetic acid caused a change in H^+ concentration, thus altering the pH value. Therefore, the change in the pH reflected the concentration of *S. typhimurium*, and could be strictly quantified with a hand-held pH meter.

Experimental section

Chemicals and reagents

ALDH and Fe_3O_4 were obtained from Sigma-Aldrich, Inc. (Saint Louis, MO, USA). The aptamer of *S. typhimurium* (CTGATGTGTGGGTAGGTGTCGTTGATTTCTTC TGGTGGGG) [43] was synthesized by Sangon Biotech Co., Ltd. (Shanghai, China). Acetaldehyde was obtained from Sangon Biotech Co., Ltd. (Shanghai, China). 2-Hydroxy-1-

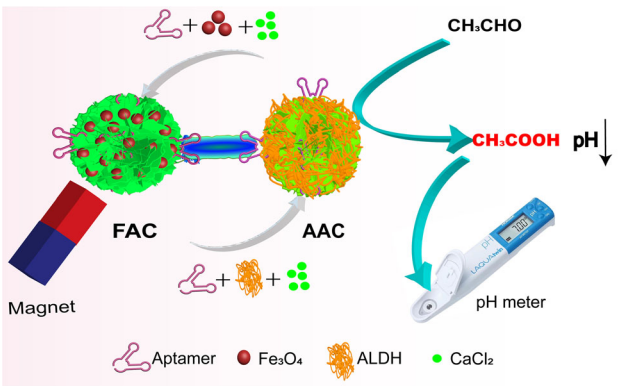

Scheme 1 Schematic illustration of the synthesis of FAC and AAC and formation of the sandwich structure for *S. typhimurium* detection.

ethanethiol (β-CH_2OHCH_2OSH) was purchased from Beijing Dingguo Changsheng Biotech Co., Ltd. (Beijing, China), and $CaCl_2$•$2H_2O$ was bought from Shantou Xilong Chemical Factory, Guangdong (Shantou, China). 10 × PBS consisted of 10 mM NaH_2PO_4 and 10 mM Na_2HPO_4, and 1 × PBS consisted of 1 mM NaH_2PO_4, 1 mM Na_2HPO_4, and 100 mM KCl. Acetaldehyde-based substrate reaction solution comprised 2 mM CH_3CHO, 10 mM β-CH_2OHCH_2OSH, and 500 mM KCl (pH 8.5). Strains of *Staphylococcus aureus* (*S. aureus*, CICC 21600), *Listeria monocytogenes* (*L. monocytogenes*, CICC 21529), *S. typhimurium* (CICC 24119), and *Escherichia coli* O157:H7 (*E. coli* O157:H7, CICC 21530) were kindly provided by China Center of Industrial Culture Collection (Beijing, China). The pH meter (B-713) used in this work was purchased from HORIBA Co., Ltd. (Kyoto, Japan) and was employed for pH measurements during quantitative detection. All the analytical pure chemicals were not further purified, and all aqueous solutions were prepared from ultrapure water (18.3 MΩ. cm, Milli-Q; Millipore, Billerica, MA, USA).

Synthesis of FAC and AAC

FAC and AAC nanocomposites were prepared in a 1.5-mL Eppendorf tube, according to previous studies, with some modifications [31, 42]. For the synthesis of FAC, 20 μL of $CaCl_2$ aqueous solution (200 mM) was added to 800 μL of PBS (pH 7.4) containing 8 μL of aptamer (10 μM) and 40 μL of Fe_3O_4 (50 mg/mL), immediately mixed by shaking, and then incubated at 25 °C for 18 h. The FAC nanocomposites were harvested by magnetic separation, washed thrice, and resuspended in 200 μL of 1 × PBS (pH 7.4). For the synthesis of AAC, 800 μL of 10 × PBS (pH 8.5) were added to 50 μL of KCl (100 mM) and 10 μL of β-CH_2OHCH_2OSH solution (1 M) to prepare antioxidant phosphate buffer. Then, 80 μL of ALDH (5 mg/mL) and 20 μL of aptamer (10 μM) were added to the phosphate buffer and mixed well. Subsequently, 20 μL of $CaCl_2$ aqueous solution (200 mM) was added to the mixing buffer, mixed gently, and incubated at room temperature for 12 h. The AAC nanocomposites were centrifuged (10,000 rpm, 6 min), washed with 1 × PBS (pH 7.4), resuspended in 200 μL of 1 × PBS (pH 7.4), and stored at 4 °C for subsequent use.

Characterization of FAC and AAC

The synthesized FAC and AAC nanocomposites were characterized by scanning electron microscopy (SEM, Hitachi su8010, Tokyo, Japan), X-ray diffraction (XRD, XD6, Beijing, China), and energy-dispersive X-ray spectrometer (EDS, USA). For SEM and EDS analyses, the suspensions of FAC and AAC were dried on the conductive film and sprayed with gold coating. For XRD analysis, the FAC and AAC suspensions were dried at 37 °C, and the respective precipitates were collected and separately ground into fine powders.

Detection of *S. typhimurium*

A total of 5 μL of FAC and 20 μL of AAC were simultaneously added into 50 μL of 1 × PBS (pH 7.4) containing different concentrations of *S. typhimurium* and incubated at 37 °C for 20 min to form FAC-target bacteria-AAC sandwich immunocomplex. The sandwich immunocomplex was separated by magnet and washed twice with 50 μL of 1 × PBS (pH 8.5), and then mixed with 100 μL of acetaldehyde-based substrate reaction solution and incubated at 45 °C for 30 min. Subsequently, the supernatant pH was detected using a portable pH meter. The registered change in pH value (ΔpH) as a signal was relative to the amount of *S. typhimurium*. The ΔpH was defined as the difference between the pH signals recorded by the pH meter in the presence and absence of the target bacteria. All the data were obtained from measurements performed in triplicate.

Determination of milk samples

For recovery analysis, the *S. typhimurium* suspensions were added to sterilized milk samples to achieve bacterial densities of 10^5, 10^6, and 10^7 CFU/mL, respectively. All the milk samples were processed according to the abovementioned testing procedure for *S. typhimurium*. The recovery (%) of *S. typhimurium* in milk samples was analyzed based on calibration plot.

Results and discussion

Characterization of FAC and AAC

Low-resolution SEM images clearly revealed that the FAC (Fig. 1a) and AAC (Fig. 1c) nanocomposites were uniform porous spheres with a diameter of about 2 μm, whereas high-resolution SEM images demonstrated interlaced peony-like flower morphology, which can effectively increase specific surface area. As shown in Fig. 1 b, a large number of Fe_3O_4 nanoparticles could be observed from the partial zoom image of FAC. Figure 1 d exhibits the dense, thick, and rough petals of AAC, and it can be presumed that the amide group of ALDH and $Ca_3(PO_4)_2$ formed complex, promoting cross-linking between the petals. During the process of petal growth, ALDH may have got attached to the petals through co-precipitation, making the petals thick and rough.

To investigate the elemental composition of FAC and AAC, EDS mapping was conducted (Fig. S1, see Electronic Supplementary Material (ESM)). As shown in Fig. S1 (see ESM), FAC was mainly composed of Fe, Ca, P, C, N, and

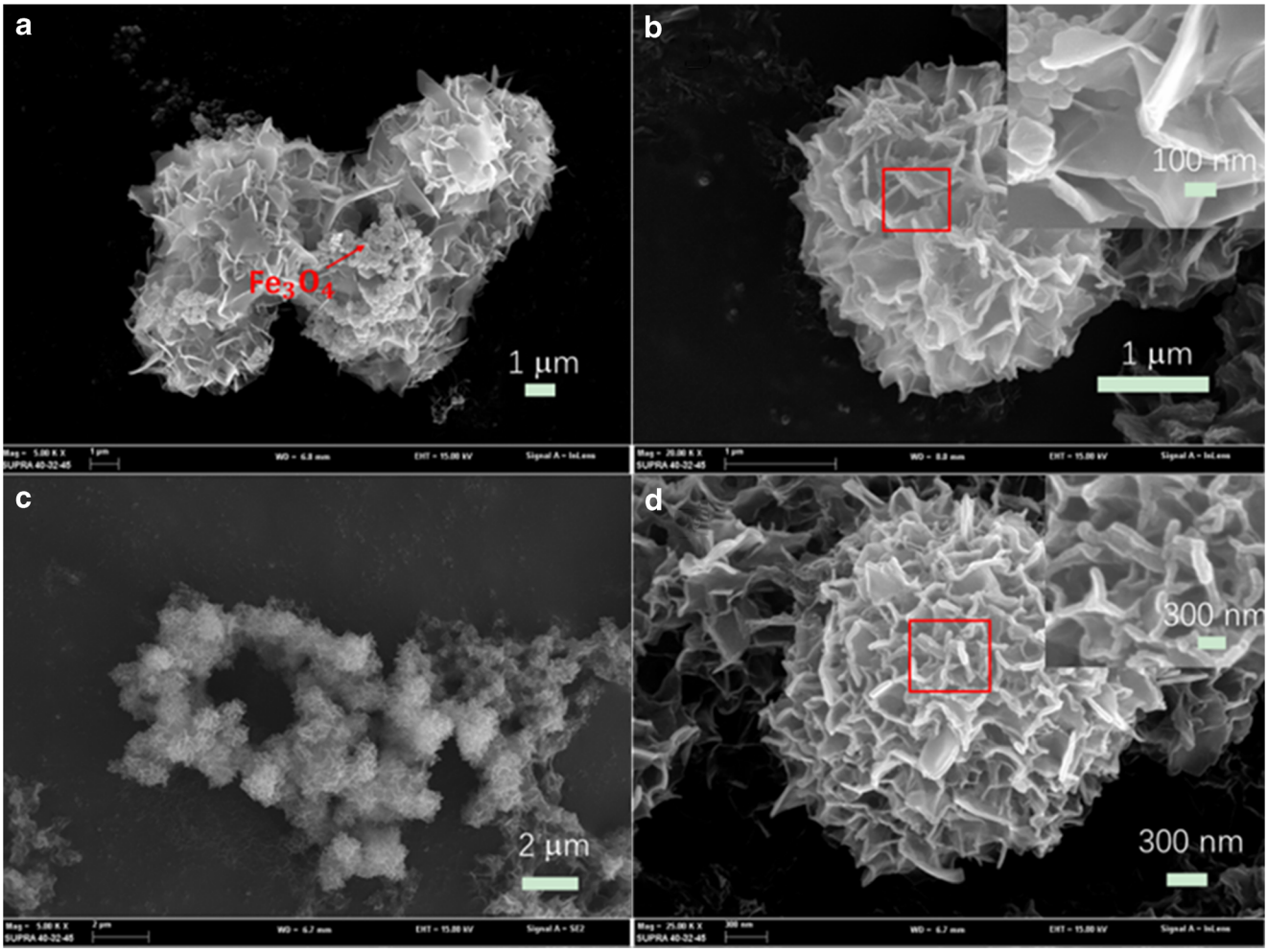

Fig. 1 SEM images of **a**, **b** FAC and **c**, **d** AAC

O elements, with Fe and N derived from Fe_3O_4 and aptamer, respectively. The EDX image showed (ESM Fig. S1b) six typical elements, including Ca, S, P, C, N, and O, in AAC, which can be attributed to $Ca_3(PO_4)_2$, ALDH, and aptamer components. Preliminary results showed that FAC and AAC nanocomposites were successfully synthesized from the corresponding components.

The XRD patterns (ESM Fig. S2a) of FAC fitted well with $Ca_3(PO_4)_2$ (JCPDS 00-018-0303) and Fe_3O_4 (JCPDS 01-077-1545) particles, confirming the inorganic component in the hybrid nanoflowers. These findings further confirmed that Fe_3O_4 particles dispersed into FAC. The XRD patterns (ESM Fig. S2b) of AAC revealed that the relative intensities and positions of all the diffraction peaks corresponded to $Ca_3(PO_4)_2$, which further proved the successful synthesis of FAC and AAC with the corresponding functional groups.

Optimization of experimental conditions

To achieve sensitive performance of the biosensor, some important experimental parameters were optimized. First, the signal probe AAC was ensured to effectively catalyze the conversion of acetaldehyde into acetic acid, generating maximum signal value of ΔpH. The amount of ALDH (0.1~0.5 mg) and aptamer (4~24 μL) embedded in AAC directly affected the signal amplification effect of the biosensor. As presented in Fig. S3a (see ESM), with the increase in the amount of ALDH, the signal value of ΔpH gradually increased. When the amount of ALDH was 0.4 mg, the signal value of ΔpH reached the maximum and then decreased. Excessive ALDH may hinder the formation of flower-like nanocomplexes, and produce tiny petals, leading to nonspecific adsorption and weak response signals. Therefore, 0.4 mg of ALDH was selected as the optimal dosage for synthesizing AAC. As shown in Fig. S3b (see ESM), the ΔpH presented a function related to the volume of the aptamer used to synthesize AAC. When the volume of the aptamer was 20 μL, maximum ΔpH value was obtained. Therefore, 20 μL was selected as the optimum aptamer volume for the synthesis of AAC. Nucleic acid aptamers are inherently acidic to a certain extent, and AAC synthesis requires weak alkaline conditions. When excess aptamers are added, the pH of the reaction system is

reduced, thus inhibiting the growth of AAC. Furthermore, as the amount of aptamer embedded in FAC determines the ability of FAC to capture the target bacteria, the volume of aptamers in FAC was also optimized. As shown in Fig. S3c (see ESM), with the increasing volume of the aptamer from 2 to 12 μL, the ΔpH value also increased until a plateau appeared at 8 μL. Therefore, 8 μL was selected as the optimal aptamer volume for the synthesis of FAC.

Subsequently, the incubation time of the sandwich immunocomplex formed by AAC, target bacteria, and FAC was optimized. The incubation time ranged from 20 to 60 min, and the signal value of ΔpH was almost a plateau and began to decline after 60 min. Hence, 20 min was selected as the best incubation time for the formation of sandwich complex (ESM Fig. S3d). In addition, we optimized the catalyzing time for the conversion of acetaldehyde into acetic acid by the signal probe AAC. As shown in Fig. S3e (see ESM), the signal value of ΔpH gradually increased from 10 to 30 min, reached a plateau from 30 to 50 min, and then decreased after 50 min. Therefore, we chose 30 min as the optimal catalyzing time. As presented in Fig. S3f (see ESM), the optimal reaction temperature was 45 °C depending on the maximal signal value of ΔpH.

When compared with some previous similar approaches, the detection time performance of the developed biosensor is superior, with the detection method requiring only 50 min for efficient completion, which is comparatively faster than the other methods (Table 1). In the developed biosensor, FAC, *S. typhimurium*, and AAC are incubated together for 20 min, and ALDH of AAC could catalyze rapid oxidation of acetaldehyde into acetic acid in 30 min. The developed immunosensor is a simple and quick method for detecting pathogenic bacteria. In a previous study, Ye et al. [31] developed organic-inorganic nanocomposites as signal tags for detecting *E. coli* O157:H7, combined with a pH meter or PGM to read the signals, which required 175 and 115 min for efficient detection, respectively. The 96-well plates fixed with *E. coli* O157:H7 antibodies were successively incubated with the target bacterium *E. coli* O157:H7 and signal label nanocomposites, which catalyzed the reaction of the substrate to produce corresponding signal. Thus, this method is time-consuming and relatively complex. Similarly, the immunosensor established by Bai et al. [42] is mainly based on immunomagnetic nanocomposites, signal label nanocomposites, and PGM readout. Although the entire procedure is relatively simple, the formation of sandwich structure of immunomagnetic nanocomposites, target bacteria, signal label nanocomposites, and enzymatic substrate of signal tags nanocomposites requires up to 115 min.

Sensitivity

The ΔpH of the proposed biosensor was assayed under optimal conditions with different concentrations of *S. typhimurium*. As shown in Fig. 2, the signal value of ΔpH showed a linear relationship with the concentration (logarithm) of *S. typhimurium* in the range of 10^2–10^8 CFU/mL. The linear regression equation is $Y = 0.252X - 0.287$ ($R^2 = 0.9856$), where Y, X, and R^2 represent ΔpH, *S. typhimurium* concentration (logarithm), and correlation coefficient, respectively. The limit of detection (LOD) was calculated as 46 CFU/mL, which generated a signal of ≥ 3 SD above the mean of the negative control values. These results demonstrated that the established biosensor has satisfactory sensitivity, large linear range, and low LOD. The sensitivity of the developed biosensor is almost the same or better than that of some previously reported methods (Table 1). When compared with the other detection methods, the developed

Table 1 Performance comparisons of different methods for foodborne pathogen detection

Target Bacterium	Methods	Linear range (CFU/mL)	LOD (CFU/mL)	Total detection time (min)	Reference
E. coli O157:H7	ELISA based on nanocomposite signal tags and pH meter readout	10^1–10^6	10	175	[31]
E. coli O157:H7	ELISA based on nanocomposite signal tags and PGM readout	10^1–10^5	10	115	[41]
S. typhimurium	Sandwich immunoassay based on magnetic nanocomposites, signal tags nanocomposites, and PGM readout	10^1–10^7	10	115	[42]
E. coli O157:H7	Sandwich immunoassay based on magnetic beads, gold nanoparticles, and electrochemical readout	10^2–10^5	148	75	[11]
E. coli O157:H7	Ferrocene antimicrobial peptide-modified biosensor	10^3–10^8	10^3	90	[10]
S. typhimurium	Immunomagnetic nanomaterials and thermal sensor readout	3×10^2–10^3	3×10^2	90	[8]
S. typhimurium	Sandwich immunoassay based on magnetic nanocomposites, signal tag nanocomposites, and pH readout	10^2–10^8	46	50	This work

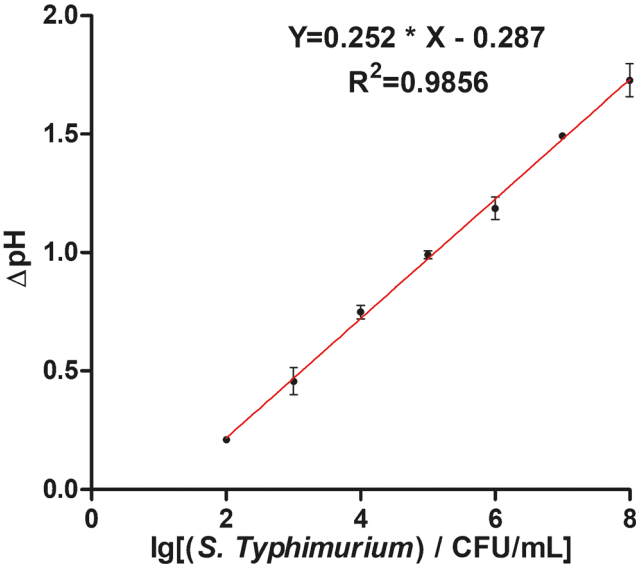

Fig. 2 Linear regression equation for *S. typhimurium* detection

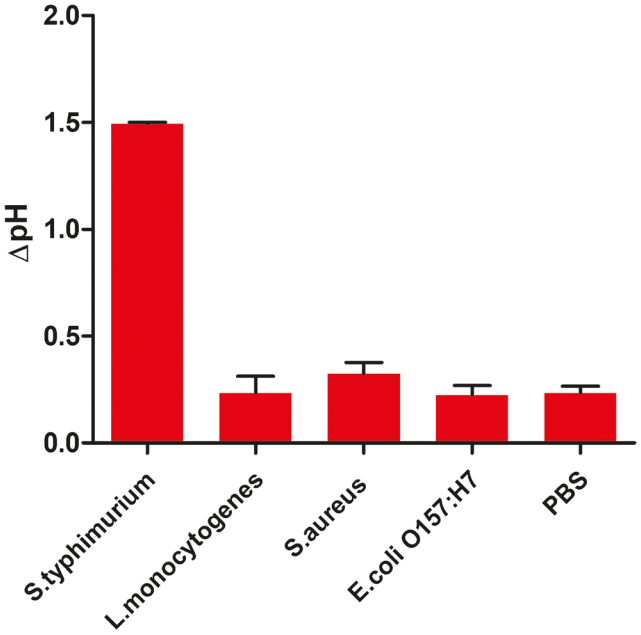

Fig. 3 Specificity assay using different pathogenic bacteria. The density of pathogenic bacteria was 1×10^7 CFU/mL

method and those of Ye et al. [31, 41] and Bai et al. [42] have low LOD. The sensitivity of our developed method is 46 CFU/mL, which is at least 1–2 orders of magnitude higher than that of conventional detection methods. It must be noted that the enzyme activity and stability in the nanocomposites enhance with increasing number of enzymes embedded in the nanocomposites, which promote signal amplification efficiency of the signal tag nanocomposites. For signal reading using a glucose meter, a glucose meter strip is essential, which increases the cost of the detection method.

The deteriorated stability at the elevated temperatures and inactivity in the organic medium limit wide application of natural enzyme. The immobilization of enzyme in organic-inorganic nanocomposites provides it with a much higher stability compared with the free form of enzyme due to the unique hierarchical nanostructure. The developed biosensor has good stability. Therefore, the developed biosensor based on enzyme embedded in organic-inorganic nanocomposite has better stability than conventional technologies (e.g., enzyme-linked immunosorbent assay) using free enzyme [44]. AAC and FAC organic-inorganic nanocomposites are both much easier to prepare (one-step co-precipitation method) and do not need any complex covalent modification. The hand-held pH meter read signal at no cost. All of these make the developed biosensor more cost-effective than traditional technologies (e.g., enzyme-linked immunosorbent assay and lateral flow).

Specificity

To assay the specificity of the developed biosensor for detecting *S. typhimurium*, several control pathogenic bacteria, such as *L. monocytogenes*, *S. aureus*, and *E. coli* O157:H7, were used to challenge the detection approach. As shown in Fig. 3, under the same experimental conditions, the signal response of the target bacteria presented a significant change, when compared with other pathogenic bacteria. These results effectively demonstrated the good specificity of the established approach. However, the practical application of the developed biosensors remains challenging and requires more efficient strategies to simplify the experimental process.

Detection of *S. typhimurium* in milk

To further investigate its capability to determine foodborne pathogens, the fabricated biosensor was used to detect real food samples. Different concentrations of *S. typhimurium* were respectively added into sterilized milk samples, and then recovery was assayed using the developed method. As presented in Table 2, the range of analytical recoveries was from 91.4 to 106.6%, which were within the acceptable criteria for bioanalytical method validation. The most important requirements are the detection limit (1 CFU/25 g) for *S. typhimurium* in milk powder [45, 46]. These results revealed that the fabricated biosensor is an excellent tool for assaying pathogenic bacteria in milk.

Conclusion

In summary, based on ALDH signaling system and portable pH meter readout, a novel signal sensing platform was fabricated for detecting *S. typhimurium*. To the best of our knowledge, this is the first study to employ ALDH as a signal detection platform for the determination of pathogenic bacteria.

Table 2 Recoveries of *S. typhimurium* from spiked milk sample

Original bacterial concentration (CFU/mL)	Added bacterial concentration (CFU/mL)	Detection (CFU/mL)	Recovery (%)
0	10^5	$(1.066 \pm 0.07) \times 10^5$	106.6 ± 7
0	10^6	$(0.914 \pm 0.05) \times 10^6$	91.4 ± 5
0	10^7	$(1.028 \pm 0.06) \times 10^7$	102.8 ± 6

With its excellent signal amplification efficiency and portable pH meter readout, the developed method presented three advantages. First, the detection method only needs 50 min for efficient completion, which is relatively faster than the other reported methods. Second, the sensitivity of 46 CFU/mL is at least an order of magnitude or 1–2 orders of magnitude higher than that of conventional detection method, which guarantees effectiveness and feasibility of the fabricated detection method. Finally, the developed biosensor can be extended to detect other pathogens by simply replacing the corresponding aptamer. Overall, the fabricated biosensor shows strong application potential in food safety and clinical diagnosis.

Funding This work was financially supported by the National Key Research and Development Program of China (No. 2016YFD0501001).

Compliance with ethical standards

Conflict of interest The authors declare that they have no competing interests.

References

1. Tang L, Li J. Plasmon-based colorimetric nanosensors for ultrasensitive molecular diagnostics. ACS Sens. 2017;2(7):857–75. https://doi.org/10.1021/acssensors.7b00282.
2. Wongkaew N, Simsek M, Griesche C, Baeumner AJ. Functional nanomaterials and nanostructures enhancing electrochemical biosensors and lab-on-a-chip performances: recent progress, applications, and future perspective. Chem Rev. 2019;119(1):120–94. https://doi.org/10.1021/acs.chemrev.8b00172.
3. Wang X, Yan C, Wang X, Zhao X, Shi C, Ma C. Integrated silica membrane-based nucleic acid purification, amplification, and visualization platform for low-cost, rapid detection of foodborne pathogens. Anal Bioanal Chem. 2020. https://doi.org/10.1007/s00216-020-02823-1.
4. Hofmann C, Kaiser B, Maerkl S, Duerkop A, Baeumner AJ. Cationic liposomes for generic signal amplification strategies in bioassays. Anal Bioanal Chem. 2020;412(14):3383–93. https://doi.org/10.1007/s00216-020-02612-w.
5. Liu D, Wang J, Wu L, Huang Y, Zhang Y, Zhu M, et al. Trends in miniaturized biosensors for point-of-care testing. TrAC Trends Anal Chem. 2020;122:115701. https://doi.org/10.1016/j.trac.2019.115701.
6. Lisi F, Peterson JR, Gooding JJ. The application of personal glucose meters as universal point-of-care diagnostic tools. Biosens Bioelectron. 2020;148:111835. https://doi.org/10.1016/j.bios.2019.111835.
7. Liu D, Tian T, Chen X, Lei Z, Song Y, Shi Y, et al. Gas-generating reactions for point-of-care testing. Analyst. 2018;143(6):1294–304. https://doi.org/10.1039/c8an00011e.
8. Zhang Z, Wang Q, Han L, Du S, Yu H, Zhang H. Rapid and sensitive detection of Salmonella typhimurium based on the photothermal effect of magnetic nanomaterials. Sens Actuators B Chem. 2018;268:188–94. https://doi.org/10.1016/j.snb.2018.04.043.
9. Bu SJ, Wang KY, Bai HS, Leng Y, Ju CJ, Wang CY, et al. Immunoassay for pathogenic bacteria using platinum nanoparticles and a hand-held hydrogen detector as transducer. Application to the detection of *Escherichia coli* O157:H7. Mikrochim Acta. 2019;186(5):296. https://doi.org/10.1007/s00604-019-3409-6.
10. Li Y, Afrasiabi R, Fathi F, Wang N, Xiang C, Love R, et al. Impedance based detection of pathogenic E. coli O157:H7 using a ferrocene-antimicrobial peptide modified biosensor. Biosens Bioelectron. 2014;58:193–9. https://doi.org/10.1016/j.bios.2014.02.045.
11. Hassan AR, de la Escosura-Muniz A, Merkoci A. Highly sensitive and rapid determination of Escherichia coli O157:H7 in minced beef and water using electrocatalytic gold nanoparticle tags. Biosens Bioelectron. 2015;67:511–5. https://doi.org/10.1016/j.bios.2014.09.019.
12. Vashist SK, Luppa PB, Yeo LY, Ozcan A, Luong JHT. Emerging technologies for next-generation point-of-care testing. Trends Biotechnol. 2015;33(11):692–705. https://doi.org/10.1016/j.tibtech.2015.09.001.
13. Vashist SK, Mudanyali O, Schneider EM, Zengerle R, Ozcan A. Cellphone-based devices for bioanalytical sciences. Anal Bioanal Chem. 2014;406(14):3263–77. https://doi.org/10.1007/s00216-013-7473-1.
14. Xiang Y, Lu Y. Using personal glucose meters and functional DNA sensors to quantify a variety of analytical targets. Nat Chem. 2011;3(9):697–703. https://doi.org/10.1038/nchem.1092.
15. Yan L, Zhu Z, Zou Y, Huang Y, Liu D, Jia S, et al. Target-responsive "sweet" hydrogel with glucometer readout for portable and quantitative detection of non-glucose targets. J Am Chem Soc. 2013;135(10):3748–51. https://doi.org/10.1021/ja3114714.
16. Ahn JK, Kim HY, Park KS, Park HG. A personal glucose meter for label-free and washing-free biomolecular detection. Anal Chem. 2018;90(19):11340–3. https://doi.org/10.1021/acs.analchem.8b02014.
17. Chavali R, Gunda NSK, Naicker S, Mitra S. Detection of Escherichia coli in potable water using personal glucose meters. Anal Methods. 2014;6. https://doi.org/10.1039/C4AY01249F.
18. Mousty C, Kaftan O, Prevot V, Forano C. Alkaline phosphatase biosensors based on layered double hydroxides matrices: role of LDH composition. Sens Actuators B Chem. 2008;133(2):442–8. https://doi.org/10.1016/j.snb.2008.03.001.
19. Song Y, Zhang Y, Bernard PE, Reuben JM, Ueno NT, Arlinghaus RB, et al. Multiplexed volumetric bar-chart chip for point-of-care diagnostics. Nat Commun. 2012;3:1283. https://doi.org/10.1038/ncomms2292.
20. Wang KY, Bu SJ, Ju CJ, Han Y, Ma CY, Liu WS, et al. Disposable syringe-based visual immunotest for pathogenic bacteria based on

the catalase mimicking activity of platinum nanoparticle-concanavalin a hybrid nanoflowers. Mikrochim Acta. 2019;186(2):57. https://doi.org/10.1007/s00604-018-3133-7.
21. Ding E, Hai J, Li T, Wu J, Chen F, Wen Y, et al. Efficient hydrogen-generation CuO/Co3O4 heterojunction nanofibers for sensitive detection of cancer cells by portable pressure meter. Anal Chem. 2017;89(15):8140–7. https://doi.org/10.1021/acs.analchem.7b01951.
22. Bu S, Wang K, Ju C, Han Y, Li Z, Du P, et al. A pregnancy test strip for detection of pathogenic bacteria by using concanavalin A-human chorionic gonadotropin-Cu3(PO4)2 hybrid nanoflowers, magnetic separation, and smartphone readout. Mikrochim Acta. 2018;185(10):464. https://doi.org/10.1007/s00604-018-2968-2.
23. Du S, Wang Y, Liu Z, Xu Z, Zhang H. A portable immune-thermometer assay based on the photothermal effect of graphene oxides for the rapid detection of Salmonella typhimurium. Biosens Bioelectron. 2019;144:111670. https://doi.org/10.1016/j.bios.2019.111670.
24. Han X, Lin S, Li Y, Cheng C, Han X. Near-infrared photothermal immunoassay for pancreatic cancer biomarker CA 19-9 on a digital thermometer. Anal Chim Acta. 2020;1098:117–24. https://doi.org/10.1016/j.aca.2019.11.027.
25. Wang J, Zhang S, Dai H, Zheng H, Hong Z, Lin Y. Dual-readout immunosensor constructed based on brilliant photoelectrochemical and photothermal effect of polymer dots for sensitive detection of sialic acid. Biosens Bioelectron. 2019;142:111567. https://doi.org/10.1016/j.bios.2019.111567.
26. Kwon D, Joo J, Lee S, Jeon S. Facile and sensitive method for detecting cardiac markers using ubiquitous pH meters. Anal Chem. 2013;85(24):12134–7. https://doi.org/10.1021/ac403329w.
27. Zhao M, Wang P, Guo Y, Wang L, Luo F, Qiu B, et al. Detection of aflatoxin B1 in food samples based on target-responsive aptamer-cross-linked hydrogel using a handheld pH meter as readout. Talanta. 2018;176:34–9. https://doi.org/10.1016/j.talanta.2017.08.006.
28. Zhang Y, Yang J, Nie J, Yang J, Gao D, Zhang L, et al. Enhanced ELISA using a handheld pH meter and enzyme-coated microparticles for the portable, sensitive detection of proteins. Chem Commun (Camb). 2016;52(17):3474–7. https://doi.org/10.1039/c5cc09852a.
29. Chen J, Xue H, Chen Q, Lin Y, Tang D, Zheng J. Enzyme-conjugated hybridization chain reaction for magneto-controlled immunoassay of squamous cell carcinoma antigen with pH meter. Chin Chem Lett. 2019;30(9):1631–4. https://doi.org/10.1016/j.cclet.2019.03.045.
30. Xie S, Yuan Y, Song Y, Zhuo Y, Li T, Chai Y, et al. Using the ubiquitous pH meter combined with a loop mediated isothermal amplification method for facile and sensitive detection of Nosema bombycis genomic DNA PTP1. Chem Commun (Camb). 2014;50(100):15932–5. https://doi.org/10.1039/c4cc06449f.
31. Ye R, Zhu C, Song Y, Lu Q, Ge X, Yang X, et al. Bioinspired synthesis of all-in-one organic-inorganic hybrid nanoflowers combined with a handheld pH meter for on-site detection of food pathogen. Small. 2016;12(23):3094–100. https://doi.org/10.1002/smll.201600273.
32. Wang L, Chen C, Huang H, Huang D, Luo F, Qiu B, et al. Sensitive detection of telomerase activity in cancer cells using portable pH meter as readout. Biosens Bioelectron. 2018;121:153–8. https://doi.org/10.1016/j.bios.2018.08.069.
33. Younus H, Arsalan A, Alam MF. Arsenic inhibits human salivary aldehyde dehydrogenase: mechanism and a population-based study. Chemosphere. 2020;243:125358. https://doi.org/10.1016/j.chemosphere.2019.125358.
34. Xu X, Chai S, Wang P, Zhang C, Yang Y, Yang Y, et al. Aldehyde dehydrogenases and cancer stem cells. Cancer Lett. 2015;369(1):50–7. https://doi.org/10.1016/j.canlet.2015.08.018.
35. Avramescu A, Noguer T, Avramescu M, Marty J-L. Screen-printed biosensors for the control of wine quality based on lactate and acetaldehyde determination. Anal Chim Acta. 2002;458(1):203–13. https://doi.org/10.1016/S0003-2670(01)01580-X.
36. Iitani K, Chien PJ, Suzuki T, Toma K, Arakawa T, Iwasaki Y, et al. Improved sensitivity of acetaldehyde biosensor by detecting ADH reverse reaction-mediated NADH fluoro-quenching for wine evaluation. ACS Sens. 2017;2(7):940–6. https://doi.org/10.1021/acssensors.7b00184.
37. Mitsubayashi K, Matsunaga H, Nishio G, Toda S, Nakanishi Y. Bioelectronic sniffers for ethanol and acetaldehyde in breath air after drinking. Biosens Bioelectron. 2005;20(8):1573–9. https://doi.org/10.1016/j.bios.2004.08.007.
38. Mitsubayashi K, Matsunaga H, Nishio G, Toda S, Nakanishi Y, Saito H, et al. Bio-sniffer sticks for breath analysis after drinking. Sens Actuators B Chem. 2005;108(1):660–4. https://doi.org/10.1016/j.snb.2004.11.093.
39. Liu Y, Zhao C, Zhao W, Zhang H, Yao S, Shi Y, et al. Multifunctional MnO_2-doped Fe_3O_4 nanoparticles as an artificial enzyme for the colorimetric detection of bacteria. Anal Bioanal Chem. 2020;412(13):3135–40. https://doi.org/10.1007/s00216-020-02563-2.
40. Zhu J, Wen M, Wen W, Du D, Zhang X, Wang S, et al. Recent progress in biosensors based on organic-inorganic hybrid nanoflowers. Biosens Bioelectron. 2018;120:175–87. https://doi.org/10.1016/j.bios.2018.08.058.
41. Ye R, Zhu C, Song Y, Lu Q, Ge X, Yang X, et al. One-pot bioinspired synthesis of all-inclusive protein-protein nanoflowers for point-of-care bioassay: detection of E. coli O157:H7 from milk. Nanoscale. 2016;8(45):18980–6. https://doi.org/10.1039/c6nr06870g.
42. Bai H, Bu S, Wang C, Ma C, Li Z, Hao Z, et al. Sandwich immunoassay based on antimicrobial peptide-mediated nanocomposite pair for determination of Escherichia coli O157:H7 using personal glucose meter as readout. Mikrochim Acta. 2020;187(4):220. https://doi.org/10.1007/s00604-020-4200-4.
43. Dwivedi HP, Smiley RD, Jaykus LA. Selection of DNA aptamers for capture and detection of Salmonella Typhimurium using a whole-cell SELEX approach in conjunction with cell sorting. Appl Microbiol Biotechnol. 2013;97(8):3677–86. https://doi.org/10.1007/s00253-013-4766-4.
44. Li Y, Wu H, Su Z. Enzyme-based hybrid nanoflowers with high performances for biocatalytic, biomedical, and environmental applications. Coord Chem Rev. 2020;416:213342. https://doi.org/10.1016/j.ccr.2020.213342.
45. Silva NFD, Magalhães JMCS, Freire C, Delerue-Matos C. Electrochemical biosensors for Salmonella: state of the art and challenges in food safety assessment. Biosens Bioelectron. 2018;99:667–82. https://doi.org/10.1016/j.bios.2017.08.019.
46. Eijkelkamp JM, Aarts HJM, van der Fels-Klerx HJ. Suitability of rapid detection methods for Salmonella in poultry slaughterhouses. Food Anal Methods. 2009;2(1):1–13. https://doi.org/10.1007/s12161-008-9040-5.